PLANE WAVE DIFFRACTION BY A STRIP WITH DIFFERENT SURFACE IMPEDANCES: PART II — THE CASE OF H POLARIZATION

Teruhisa Tsushima[1)]*, Kazuya Kobayashi[1)], Eldar I. Veliev[2)], and Shoichi Koshikawa[3)]

[1)] Department of Electrical and Electronic Engineering, Chuo University
1-13-27 Kasuga, Bunkyo-ku, Tokyo 112-8551, Japan
[2)] Institute of Radiophysics and Electronics, National Academy of Sciences
Ulitsa Proskury 12, Kharkov 310085, Ukraine
[3)] Antenna Giken Co., Ltd., 4-72 Miyagayato, Omiya 330-0011, Japan

1. Introduction

The scattering from imperfectly conducting and absorbing strips is an important subject in antenna and radar cross section (RCS) studies since this geometry serves as a suitable model of finite metal-backed dielectric layers and dielectric-coated wires. The diffraction by strips with impedance and related approximate boundary conditions has been investigated thus far using function-theoretic and high-frequency methods [1–3]. In Part I [4] of this two-part paper, we have considered a two-dimensional (2-D) strip with different impedances on its two surfaces, and solved the E-polarized plane wave diffraction rigorously using the analytical-numerical approach [5]. This approach is based on the orthogonal polynomial expansion in conjunction with the Fourier transform, and is different from the methods employed previously for analyzing scattering problems related to the impedance strip. In this second part, we shall analyze the diffraction problem involving the same impedance strip as in [4] for the H-polarized plane wave incidence by means of the analytical-numerical approach.

Applying the boundary condition to an integral representation of the scattered field, the problem is formulated in terms of simultaneous integral equations satisfied by the current density functions. The integral equations are reduced to two infinite systems of linear algebraic equations (SLAE) using a method similar to that employed for the E-polarized case [4], which are solved numerically with high accuracy via a truncation procedure. Physical quantities are then expressed in terms of the solution of the SLAE. Illustrative numerical examples on the monostatic and bistatic RCS are presented, and the far field scattering characteristics are discussed. Some comparisons with Tiberio *et al.* [3] are given to validate the present method.

In the following, we shall use abbreviated citation of equations in Part I such as (I.1) if necessary, where the prefix I and the second number in the parentheses denote Part I and the equation number, respectivery. The time factor is assumed to be $e^{-i\omega t}$ and suppressed throughout this paper.

2. Formulation of the Problem

We consider a 2-D impedance strip of zero thickness illuminated by an H-polarized plane wave, as shown in Fig. 1, where ζ_1 and ζ_2 denote the normalized impedance of the upper and lower surfaces of the strip, respectively. Let the total magnetic field be

$$H_z(x,y) = H_z^i(x,y) + H_z^s(x,y), \tag{1}$$

where

$$H_z^i(x,y) = e^{-ik\left(x\alpha_0 + y\sqrt{1-\alpha_0^2}\right)}, \quad \alpha_0 = \cos\theta \tag{2}$$

is the incident field for $0 \le \theta \le \pi$ with $k = \omega\sqrt{\mu_0\varepsilon_0}$ being the free-space wavenumber. The total field satisfies the boundary condition

$$\frac{\partial H_z(x,\pm 0)}{\partial y} \pm ik\zeta_{1,2} H_z(x,\pm 0) = 0 \tag{3}$$

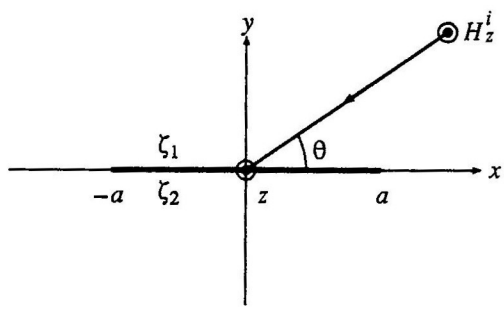

Fig. 1. Geometry of the problem.

for $|x| < a$. The scattered field $H_x^s(x,y)$ in (1) has the integral representation

$$H_x^s(x,y) = -\frac{i}{4}\int_{-a}^{a}\left\{f_1(x') + f_2(x')\frac{\partial}{\partial y}\right\} H_0^{(1)}\left(k\sqrt{(x-x')^2+y^2}\right) dx' \tag{4}$$

with $H_0^{(1)}(\cdot)$ being the Hankel function of the first kind, where $f_1(x)$ and $f_2(x)$ are the unknown magnetic and electric current density functions, respectively, which are defined by

$$f_1(x) = \frac{\partial H_z(x,+0)}{\partial y} - \frac{\partial H_z(x,-0)}{\partial y}, \quad f_2(x) = H_z(x,+0) - H_z(x,-0). \tag{5}$$

Taking into account the boundary condition as given by (3), it follows from (1), (2), and (4) that

$$-\frac{Z_1}{k}f_1(x) - Z_2 f_2(x) = 2ie^{-ikx\alpha_0} + \frac{1}{2}\int_{-a}^{a} f_1(x')H_0^{(1)}\left(k|x-x'|\right) dx', \tag{6a}$$

$$Z_2 f_1(x) + kZ_3 f_2(x) = 2k\sqrt{1-\alpha_0^2}e^{-ikx\alpha_0} + \frac{1}{2}\lim_{y\to 0}\frac{\partial^2}{\partial y^2}\int_{-a}^{a} f_2(x')H_0^{(1)}\left(k\sqrt{(x-x')^2+y^2}\right) dx', \tag{6b}$$

where

$$Z_1 = \frac{2}{\zeta_1+\zeta_2}, \quad Z_2 = \frac{i(\zeta_1-\zeta_2)}{\zeta_1+\zeta_2}, \quad Z_3 = \frac{2\zeta_1\zeta_2}{\zeta_1+\zeta_2}. \tag{7}$$

Equations (6a,b) are the integral equations satisfied by the current density functions.

3. Solution of the Integral Equations

We take the finite Fourier transform of (6a,b) with respect to x over the range $|x| < a$ and arrange the results with the aid of the Fourier integral representation of the Hankel function. This leads to

$$\frac{Z_1}{\kappa}F_1(\beta) + iZ_2F_2(\beta) = 4i\frac{\sin\kappa(\alpha_0+\beta)}{\kappa(\alpha_0+\beta)} + \frac{1}{\pi}\int_{-\infty}^{\infty} F_1(\alpha)\frac{\sin\kappa(\alpha-\beta)}{\kappa(\alpha-\beta)}\frac{d\alpha}{\sqrt{1-\alpha^2}}, \tag{8a}$$

$$\frac{Z_2}{\kappa}F_1(\beta) + Z_3F_2(\beta) = 4\sqrt{1-\alpha_0^2}\frac{\sin\kappa(\alpha_0+\beta)}{\kappa(\alpha_0+\beta)} - \frac{1}{\pi}\int_{-\infty}^{\infty} F_2(\alpha)\frac{\sin\kappa(\alpha-\beta)}{\alpha-\beta}\sqrt{1-\alpha^2}d\alpha \tag{8b}$$

with $\kappa = ka$, where $F_{1,2}(\alpha)$ denote the finite Fourier transforms of $f_{1,2}(x)$ in (5) (see (I.9)). As in the E-polarized case [4], $f_{1,2}(x)$ are expanded into the infinite series

$$f_1(x) = \frac{1}{a\sqrt{1-(x/a)^2}}\left\{f_0^1 + 2\sum_{n=1}^{\infty}\frac{f_n^1}{n}T_n\left(\frac{x}{a}\right)\right\}, \quad f_2(x) = \sqrt{1-\left(\frac{x}{a}\right)^2}\sum_{n=0}^{\infty} f_n^2 U_n\left(\frac{x}{a}\right) \tag{9}$$

with $f_n^{1,2}$ for $n = 0, 1, 2, \cdots$ being unknown coefficients, where $T_n(\cdot)$ and $U_n(\cdot)$ denote the Chebyshev polynomial of the first and second kinds, respectively. We now substitute (9) into (8a,b) and arrange the results. This leads to the two infinite systems of linear algebraic equations (SLAE) as in

$$-\sum_{n=0}^{\infty} x_n^1(Z_1 d_{mn}^0 + c_{mn}) - Z_2\sum_{n=0}^{\infty} x_n^2 d_{mn}^1 = 4i\gamma_m, \tag{10a}$$

$$Z_2\sum_{n=0}^{\infty} x_n^1 d_{mn}^0 + \sum_{n=0}^{\infty} x_n^2(Z_3 d_{mn}^1 + b_{mn}) = 4\sqrt{1-\alpha_0^2}\gamma_m \tag{10b}$$

for $m = 0, 1, 2, \cdots$, where

$$x_0^1 = f_0^1, \quad x_n^1 = 2(-i)^n f_n^1/n \quad \text{for} \quad n = 1, 2, 3, \cdots; \quad x_n^2 = (-i)^n(n+1)f_n^2 \quad \text{for} \quad n = 0, 1, 2, \cdots. \tag{11}$$

In (10a,b), the coefficients γ_m, b_{mn}, c_{mn}, d_{mn}^0, and d_{mn}^1 are defined by (I.13), (I.14a,b), and (I.15a,b). The unknowns $x_n^{1,2}$ can be determined by solving (10a,b) numerically via a truncation procedure.

4. Scattered Far Field

Taking into account the asymptotic expansion of the Hankel function, we find from (4) that

$$H_x^s(r,\phi) \sim \sqrt{\frac{2}{\pi kr}}e^{i(kr-\pi/4)}\Phi(\phi), \quad kr \to \infty \tag{12}$$

with (r,ϕ) being the cylindrical coordinate defined by $x = r\cos\phi$, $y = r\sin\phi$ for $-\pi \le \phi \le \pi$, where $\Phi(\phi)$ is the pattern function expressed in terms of the coefficients $x_n^{1,2}$ as follows:

$$\Phi(\phi) = -\frac{i\pi}{4}\sum_{n=0}^{\infty} x_n^1 J_n(\kappa\cos\phi) + \frac{\pi}{4}\tan\phi\sum_{n=0}^{\infty} x_n^2 J_{n+1}(\kappa\cos\phi). \tag{13}$$

Physical quantities are therefore computed by using (13).

5. Numerical Results and Discussion

We shall now discuss the far field scattering characteristics of the strip based on numerical examples of the RCS. Figure 2 shows the monostatic RCS as a function of incidence angle θ for $ka = 5.0, 15.0$, where the surface impedances ζ_1 and ζ_2 have been chosen to be the same as in the E-polarized case [4], namely, $(\zeta_1, \zeta_2) = (0.0, 0.0)$, $(1.5, 3.0)$, $(1.5, 1.5)$, $(3.0, 3.0)$. Here $\zeta_{1,2} = 0.0$ implies the case of a perfectly conducting strip. Comparing the results between the impedance and perfectly conducting strips, the RCS reduction is observed except near $\theta = 0°$ for the impedance case. In view of the three curves for the impedance strip, the RCS characteristics for the strip with different surface impedances are close to the results for the same impedance case with $\zeta_{1,2} = 1.5$ over $30° < \theta < 90°$ and to those with $\zeta_{1,2} = 3.0$ over $-90° < \theta < -30°$. It is therefore inferred that the difference on the surface impedance in the shadow region does not affect the backscattered far field except near the grazing incidence. We have presented in Fig. 3 the bistatic RCS as a function of observation angle ϕ for $\theta = 60°$ and $ka = 5.0, 15.0$. It is seen that the RCS of the impedance strip is lower than the perfectly conducting case for $-40° < \theta < 170°$ with $\theta \not\approx 0°$, whereas the results for both the perfectly conducting and impedance strips show close features in the neighborhood of the incident shadow boundary ($\phi = -120°$). Figure 4 illustrates comparison with the results obtained by Tiberio *et al.* [3] using the geometrical theory of diffraction (GTD) together with the Maliuzhinetz method, where the bistatic RCS is shown as a function of observation angle ϕ for $\theta = 180°$, $ka = 10.0$, and $(\zeta_1, \zeta_2) = (4.0, 0.0)$. We see from the figure that our RCS results agree quite well with the results presented in [3].

Acknowledgments

The authors would like to thank Mr. Masanori Ogata, a former graduate school student at Chuo University, for assisting in the preparation of the manuscript. This work was supported in part by the 1997 Chuo University Special Research Grant and by the Institute of Science and Engineering, Chuo University.

References

[1] T. B. A. Senior, "Backscattering by a resistive strip," *IEEE Trans. Antennas Propagat.*, vol. AP-27, no. 6, pp. 808–813, 1979.

[2] M. I. Herman and J. L. Volakis, "High-frequency scattering by a resistive strip and extensions to conductive and impedance strips," *Radio Sci.*, vol. 22, no. 3, pp. 335–349, 1987.

[3] R. Tiberio, F. Bessi, G. Manara, and G. Pelosi, "Scattering by a strip with two face impedances at edge-on incidence," *Radio Sci.*, vol. 17, no. 5, pp. 1199–1210, 1982.

[4] T. Tsushima, K. Kobayashi, E. I. Veliev, and S. Koshikawa, "Plane wave diffraction by a strip with different surface impedances: part I — the case of E polarization," to be presented at *1998 Korea-Japan AP/EMC/EMT Joint Conference*, September 3–5, 1998, Pusan, Korea.

[5] E. I. Veliev and V. V. Veremey, "Numerical-analytical approach for the solution to the wave scattering by polygonal cylinders and flat strip structures," in *Analytical and Numerical Methods in Electromagnetic Wave Theory*, Chap. 10, M. Hashimoto, M. Idemen, O. A. Tretyakov, Eds., Science House, Tokyo, 1993.

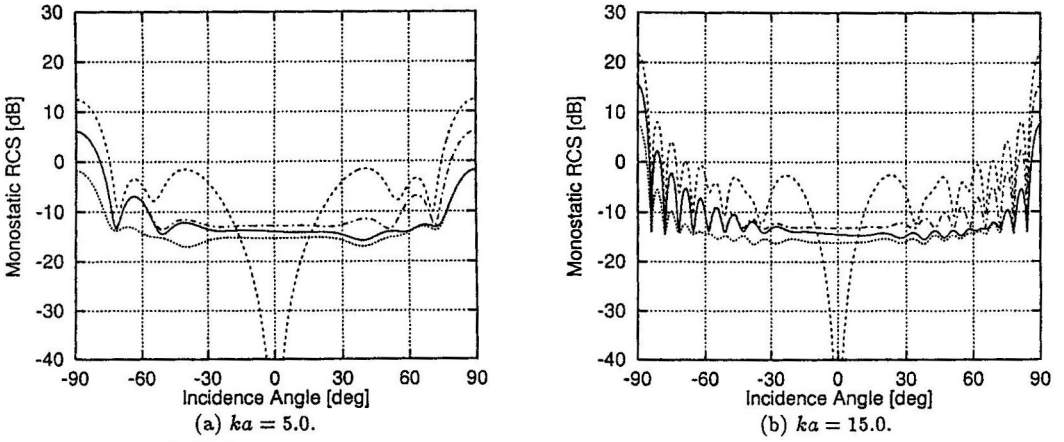

(a) $ka = 5.0$. (b) $ka = 15.0$.

Fig. 2. Monostatic RCS. – – – – – –: $\zeta_1 = \zeta_2 = 0.0$; ————: $\zeta_1 = 1.5$, $\zeta_2 = 3.0$; ·····: $\zeta_1 = \zeta_2 = 1.5$; – · – · – · –: $\zeta_1 = \zeta_2 = 3.0$.

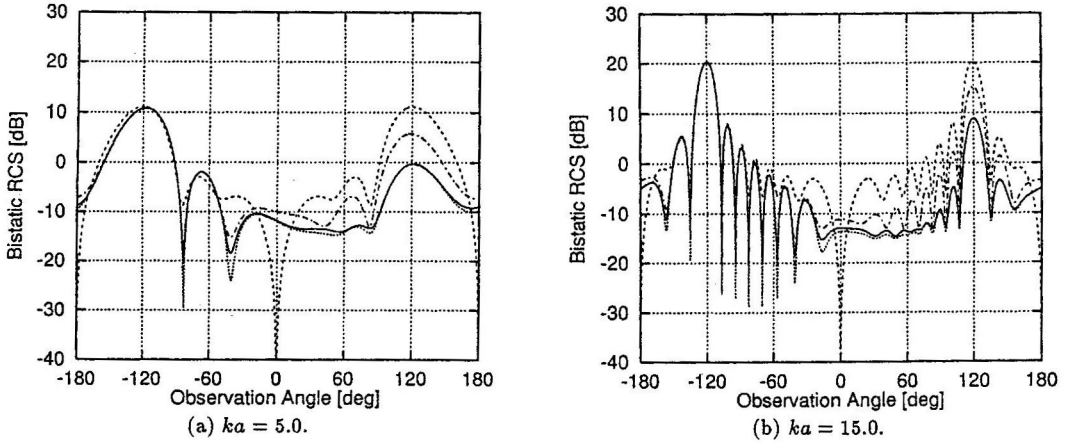

(a) $ka = 5.0$. (b) $ka = 15.0$.

Fig. 3. Bistatic RCS for $\theta = 60°$. – – – – – –: $\zeta_1 = \zeta_2 = 0.0$; ————: $\zeta_1 = 1.5$, $\zeta_2 = 3.0$; ·····: $\zeta_1 = \zeta_2 = 1.5$; – · – · – · –: $\zeta_1 = \zeta_2 = 3.0$.

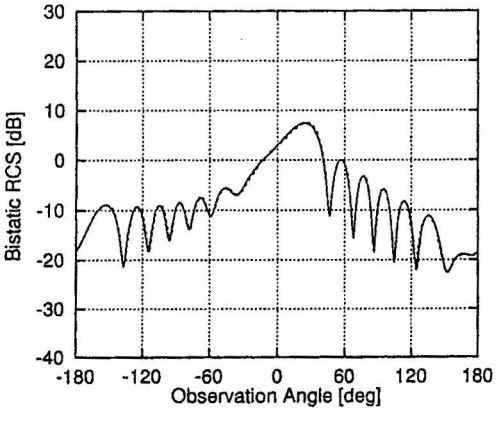

Fig. 4. Bistatic RCS for $\theta = 180°$, $ka = 10.0$, $\zeta_1 = 4.0$, $\zeta_2 = 0.0$ and its comparison with Tiberio *et al.* [3]. ————: this paper; – – – – – –: Tiberio *et al.*